Science Advances
AAAS

Supplementary Materials for

Secondary loss of *miR-3607* reduced cortical progenitor amplification during rodent evolution

Kaviya Chinnappa, Adrián Cárdenas, Anna Prieto-Colomina, Ana Villalba, Ángel Márquez-Galera, Rafael Soler, Yuki Nomura, Esther Llorens, Ugo Tomasello, José P. López-Atalaya, Víctor Borrell*

*Corresponding author. Email: vborrell@umh.es

Published 12 January 2022, *Sci. Adv.* **8**, eabj4010 (2022)
DOI: 10.1126/sciadv.abj4010

The PDF file includes:

Figs. S1 to S8
Legends for tables S1 to S3
Legends for movies S1 to S3
References

Other Supplementary Material for this manuscript includes the following:

Tables S1 to S3
Movies S1 and S2

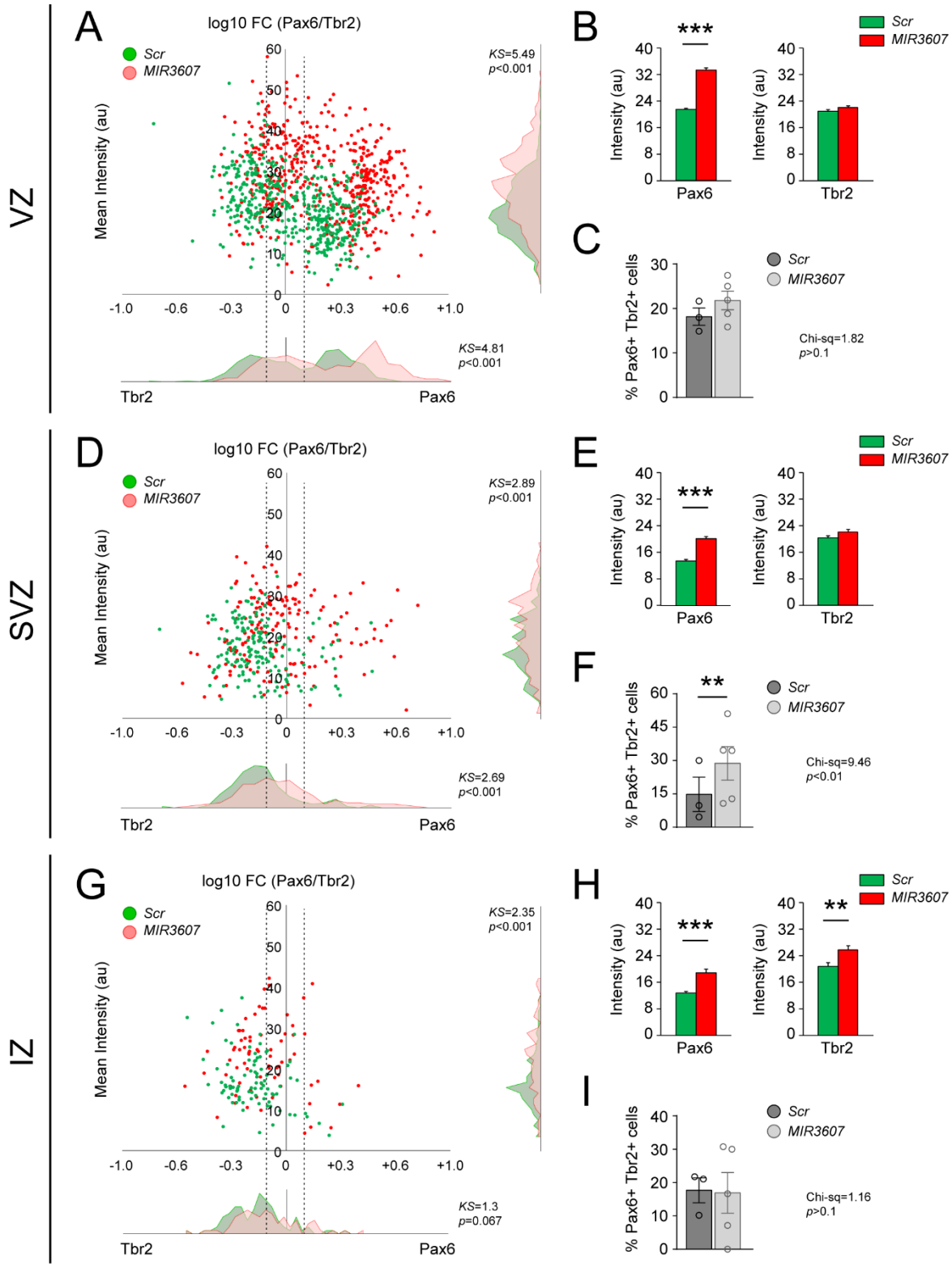
VZ
SVZ
IZ
A
log10 FC (Pax6/Tbr2)
Scr
MIR3607
Mean Intensity (au)
KS=5.49
p<0.001
KS=4.81
p<0.001
Tbr2
Pax6
B
***
Intensity (au)
Pax6
Tbr2
C
% Pax6+ Tbr2+ cells
Chi-sq=1.82
p>0.1
D
KS=2.89
p<0.001
KS=2.69
p<0.001
E
F
**
Chi-sq=9.46
p<0.01
G
KS=2.35
p<0.001
KS=1.3
p=0.067
H
I
Chi-sq=1.16
p>0.1

Fig. S1. *MIR3607* drives overexpression of Pax6 in cortical cells

(**A,D,G**) Scatter plots of ratio Pax6/Tbr2 expression level (log10 Fold Change) relative to mean intensity of both markers (arbitrary units) in individual GFP+ cells, and frequency distribution plots for each of the individual parameters, at the indicated layers of the developing cortex. Dashed vertical lines delimit Pax6/Tbr2 co-expression (-0.1<log10FC<+0.1).

(**B,E,H**) Average expression intensity of Pax6 and Tbr2 in individual cells at the indicated layers.

(**C,F,I**) Proportion of cells co-expressing Pax6 and Tbr2 (-0.1<log10FC<+0.1). Differences in Pax6 expression intensity were largest in VZ, but differences in Pax6/Tbr2 co-expression were largest in SVZ.

N = 471 cells VZ, 176 cells SVZ, 91 cells IZ, 3 embryos for *Scr*; 538 cells VZ, 176 cells SVZ, 73 cells IZ, 5 embryos for *MIR3607*. Kolmogorov-Smirnoff test (A,D,G), t-test (B,E,H), X^2 test (C,F,I); $^{**}p<0.01$, $^{***}p<0.001$.

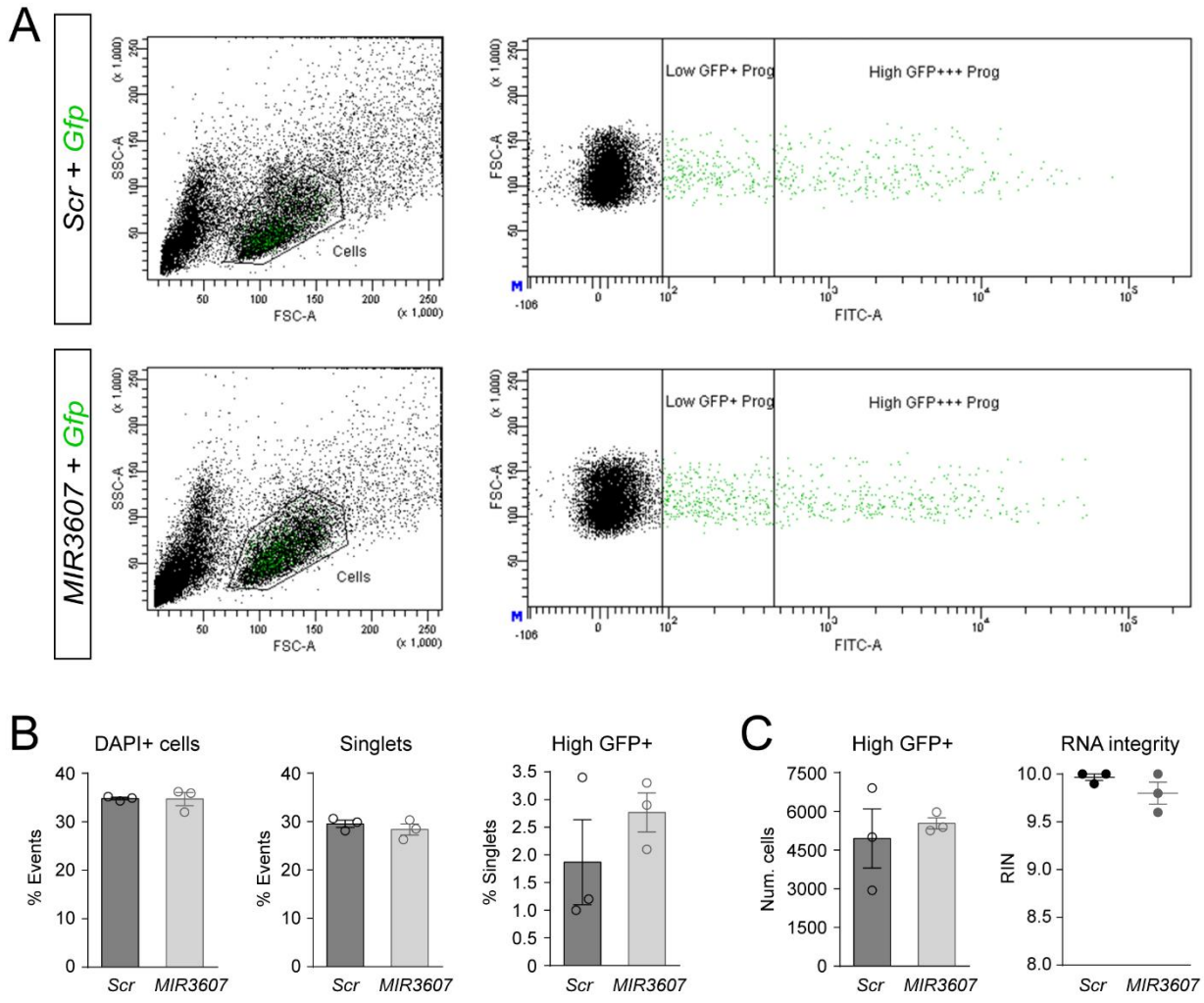

Fig. S2. FACS sorting of cortical cells for transcriptomic profiling

(**A**) Examples of sort profiles of cells from E15.5 cortex electroporated at E14.5 with the indicated plasmids. Left column shows the dot plots of cells in forward scatter (FSC) and side scatter (SCC) with the polygon indicating the gate selecting the healthy cells. Right column shows the dot plots of cells in forward scatter (FSC) with fluorescence intensity (FITC) indicated. Only High GFP+++ cells were selected for RNA-seq analysis.
(**B**) Quality control of FACS sorting, showing similar values between *Scr*- and *MIR3607*-electroporated embryos for frequency of DAPI+ elements, of singlets among total events, and frequency of high GFP+ cells among singlets.
(**C**) Quality control of RNA extraction experiments, showing a similar number of high GFP+ single cells used for RNA extraction, and similar integrity of extracted RNA between experimental groups, above 9.5 in all cases.
Histograms indicate mean ± SEM, and circles within indicate values for individual embryos; n = 3 embryos per group; X^2 tests (B) and t-tests (C) revealed non-significance (p>0.05).

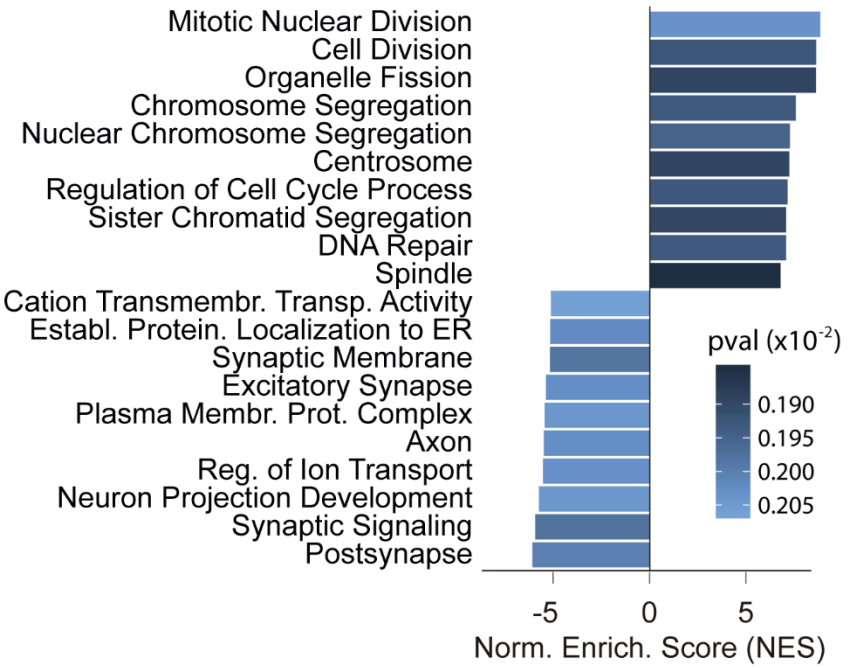

Fig. S3. Gene Ontology analysis of DEGs from GSEA

Bar chart of top ranked GO gene sets according to normalized enrichment score (NES), from gene set enrichment analysis (GSEA). Bars are color-coded according to statistical significance (nominal p value) as indicated.

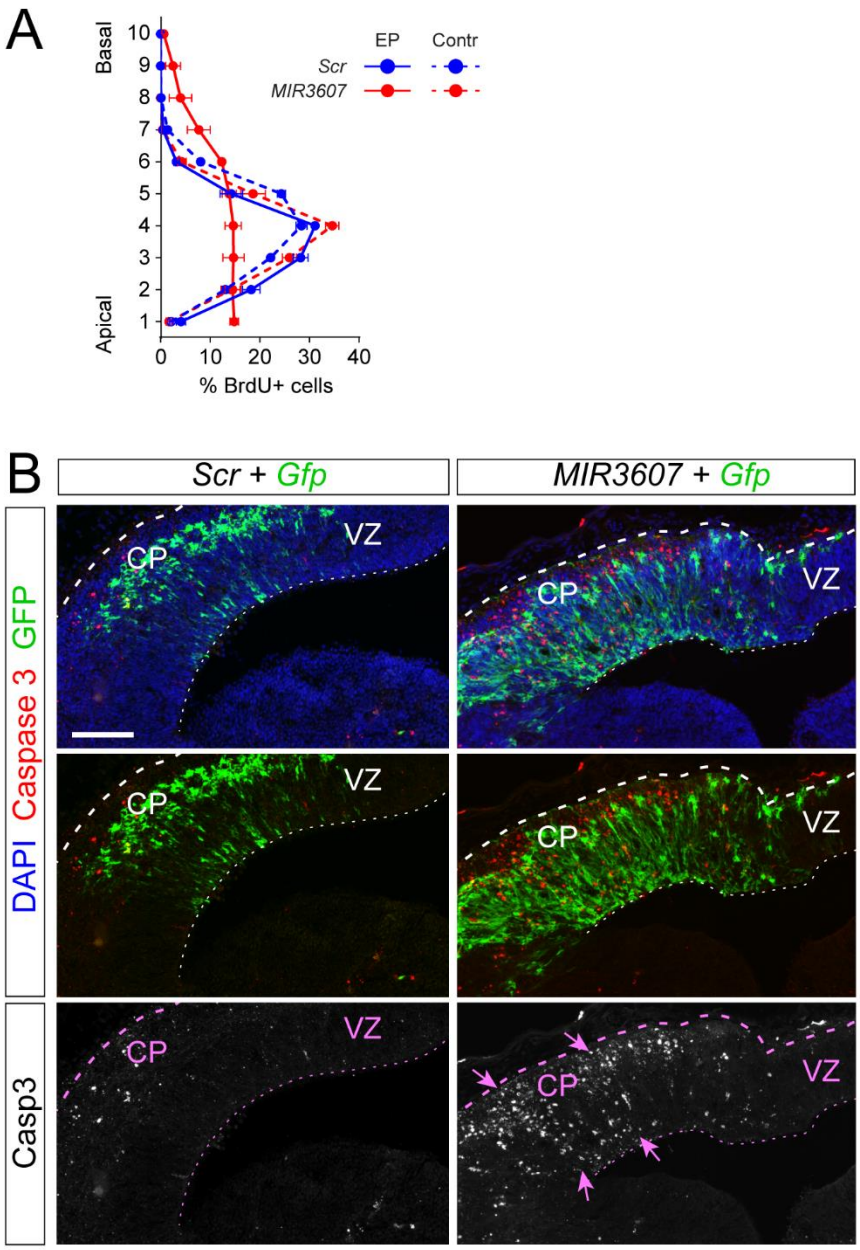

Fig. S4. *MIR3607* overexpression induces progenitor cell disorganization and apoptosis in the early embryonic mouse cortex

(**A**) Quantification of binned distribution of BrdU+ cells across the thickness of the parietal cortex of mouse embryos electroporated at E12.5 with the indicated plasmids, and analyzed at E13.5. Data is from electroporated hemispheres (solid lines) and from non-electroporated, contralateral hemispheres (dashed lines). The typical accumulation of BrdU-incorporating cells in the basal side of the VZ (bins 3-5) was observed in *Scr*-electroporated (solid blue line) and contralateral hemispheres (dashed lines), but severely disturbed in *MIR3607*-electroporated cortices (solid red line). Plots show mean ± SEM; n = 2,673 cells ipsi, 3,583 cells contra, 2 embryos, Scr; 5,150 cells ipsi, 5,485 cells contra, 4 embryos, *MIR3607*.

(**B**) Sections through the parietal cortex of mouse embryos electroporated at E12.5 with the indicated plasmids, analyzed at E13.5 and stained as indicated. Expression of *MIR3607* caused a dramatic increase in apoptosis (Casp3+ cells), both in VZ and CP (arrows). Dotted lines indicate apical surface, dashed lines indicate pial surface.
Scale bar: 100μm.

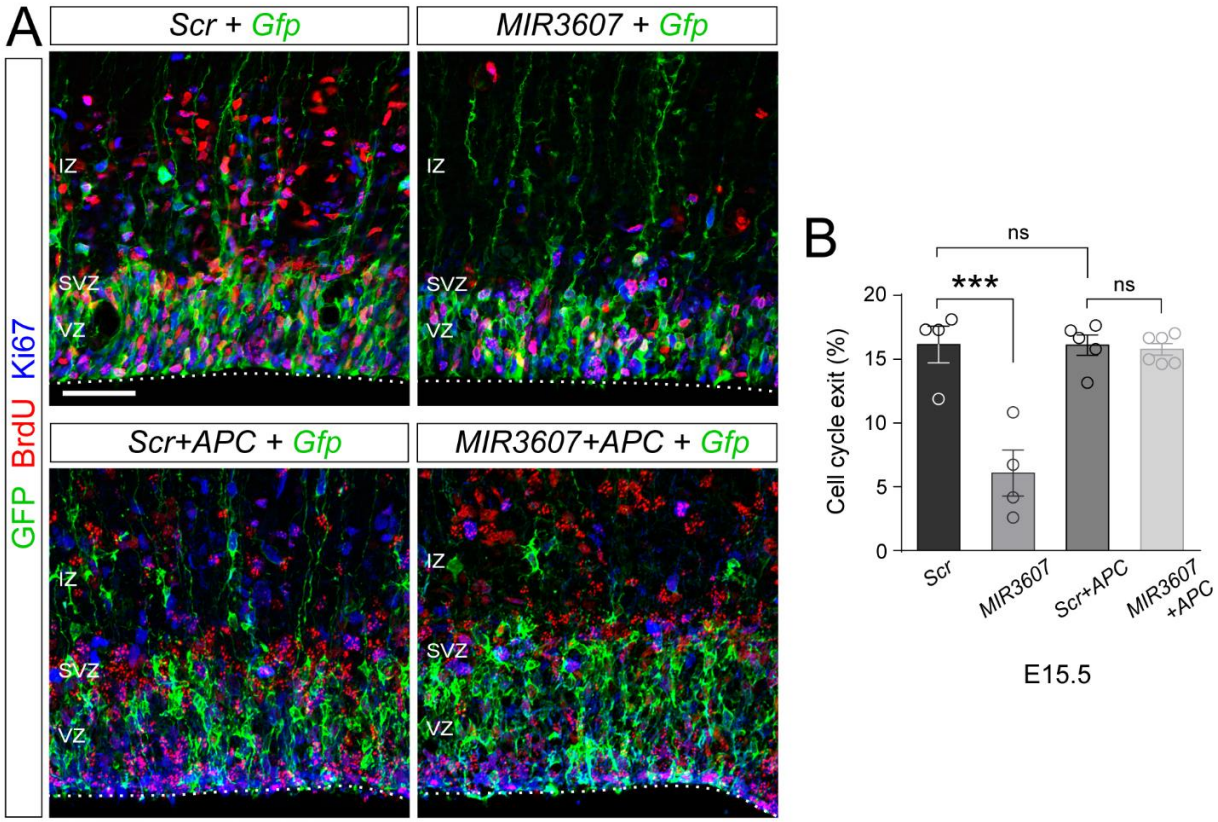

Fig. S5. Expression of *APC* rescues the changes in cell cycle exit caused by *MIR3607*
(**A,B**) Sections through the parietal cortex of E15.5 mouse embryos injected with a single pulse of BrdU at E14.5 followed 4hr later by electroporation with the indicated plasmids, and stained as indicated (A), and quantifications of cell cycle exit of GFP+ cells in any layer (B). Histograms indicate mean ± SEM, and circles within indicate values for individual embryos; *n* = 4-6 embryos per group. X^2 test; *** p<0.001; ns, not significant.

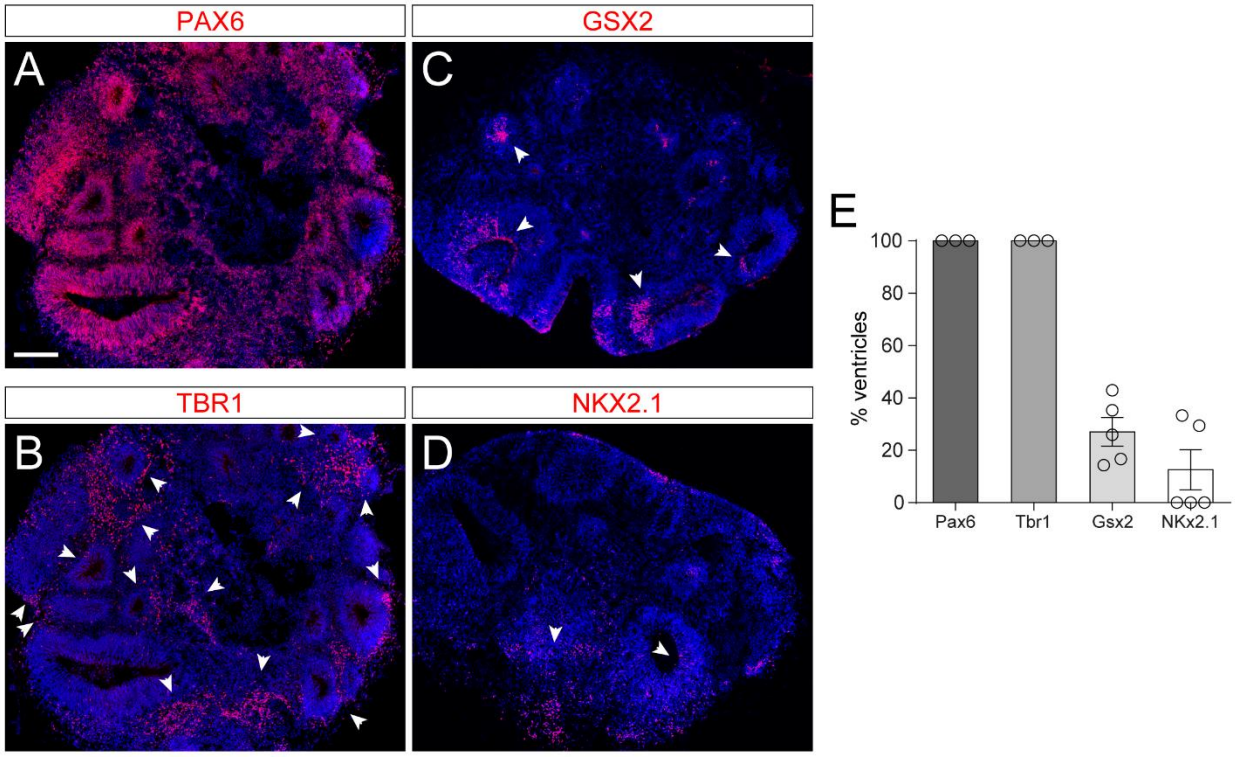

Fig. S6. Validation of cortical identity of human cerebral organoids

(**A-D**) Sections through human cerebral organoids immunostained for the indicated cortical (A,B) and subcortical (C,D) markers. Arrowheads indicate ventricles containing cells positive for the relevant marker. All ventricles are positive for the cortical markers PAX6 and TBR1, whereas only a minority have a few cells positive for the subcortical markers GSX2 and NKX2.1.

(**E**) Proportion of ventricles positive for the indicated markers within individual organoids. Histograms show mean ± SEM; circles indicate values for individual organoids; *n* = 3-5 organoids per group, 5-21 ventricles per organoid.

Scale bar: 150µm.

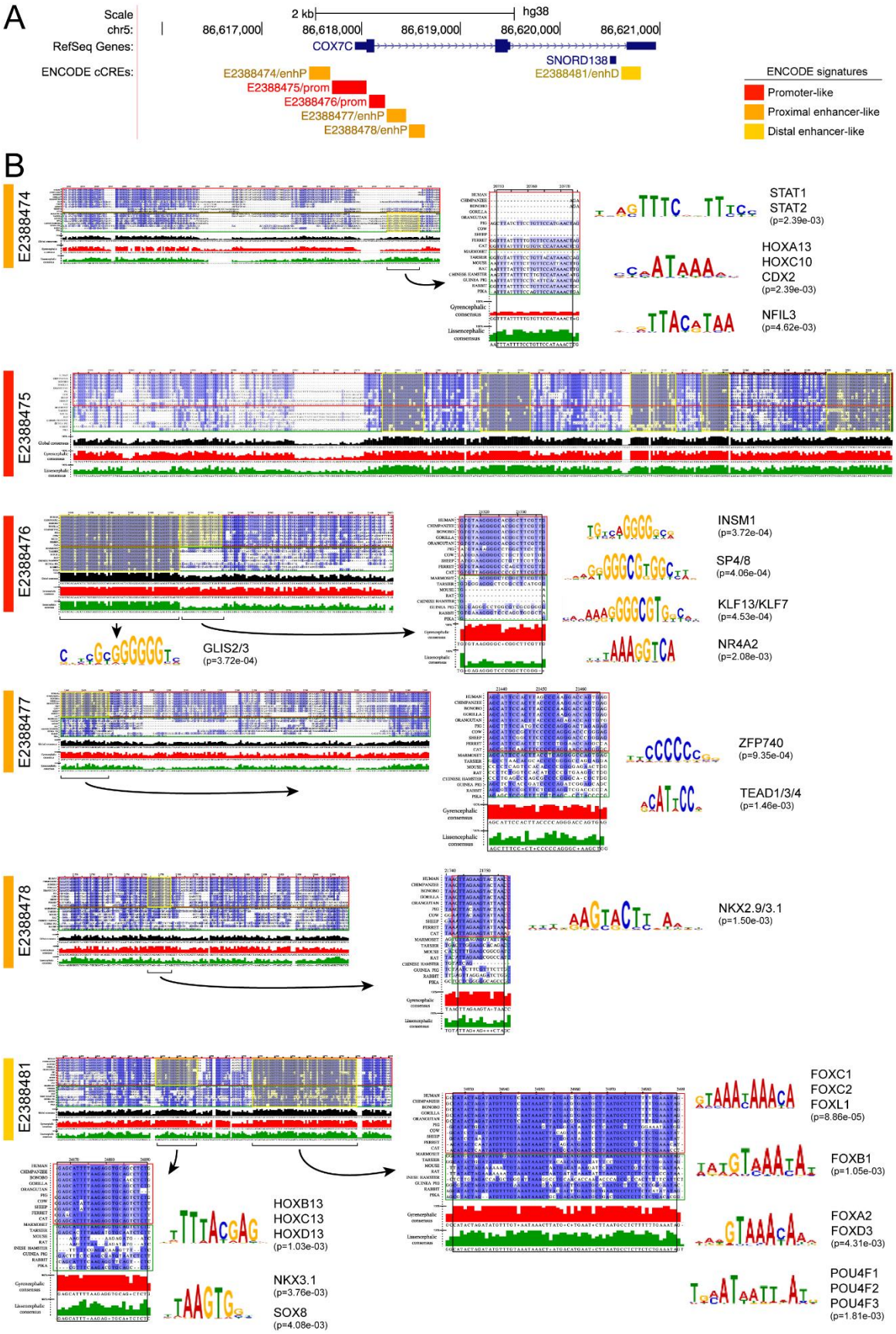
A
Scale
chr5:
RefSeq Genes:
ENCODE cCREs:
2 kb
hg38
86,617,000
86,618,000
86,619,000
86,620,000
86,621,000
COX7C
SNORD138
E2388474/enhP
E2388475/prom
E2388476/prom
E2388477/enhP
E2388478/enhP
E2388481/enhD
ENCODE signatures
Promoter-like
Proximal enhancer-like
Distal enhancer-like
B
E2388474
STAT1
STAT2
(p=2.39e-03)
HOXA13
HOXC10
CDX2
(p=2.39e-03)
NFIL3
(p=4.62e-03)
E2388475
E2388476
GLIS2/3
(p=3.72e-04)
INSM1
(p=3.72e-04)
SP4/8
(p=4.06e-04)
KLF13/KLF7
(p=4.53e-04)
NR4A2
(p=2.08e-03)
E2388477
ZFP740
(p=9.35e-04)
TEAD1/3/4
(p=1.46e-03)
E2388478
NKX2.9/3.1
(p=1.50e-03)
E2388481
HOXB13
HOXC13
HOXD13
(p=1.03e-03)
NKX3.1
(p=3.76e-03)
SOX8
(p=4.08e-03)
FOXC1
FOXC2
FOXL1
(p=8.86e-05)
FOXB1
(p=1.05e-03)
FOXA2
FOXD3
(p=4.31e-03)
POU4F1
POU4F2
POU4F3
(p=1.81e-03)

Fig. S7. Conservation and divergence of *MIR3607* expression regulation
(**A**) Genomic region of MIR3607 (SNORD138) in the human genome (GRCh38/hg38). Colored boxes indicate candidate cis-regulatory elements (cCREs) showing promoter-like, proximal enhancer-like and distal enhancer-like signatures (*67*).
(**B**) DNA sequences from -5kb to +1Kb downstream of MIR3607 TSS for 18 species, from UCSD Table browser (*xenoRefGene*). Gyrencephalic species are on top (red boxes): human (*Homo sapiens*), chimpanzee (*Pan troglodytes*), bonobo (*Pan paniscus*), gorilla (*Gorilla gorilla*), orangutan (*Pongo pygmaeus*), pig (*Sus domesticus*), cow (*Bos taurus*), sheep (*Ovis aries*), ferret (*Mustela furo*) and cat (*Felis silvestris*). Lissencephalis species are on bottom (green boxes): marmoset (*Callithrix jacchus*), tarsier (*Tarsius tarsier*), mouse (*Mus musculus*), rat (*Rattus norvegicus*), chinese hamster (*Cricetulus barabensis*), guinea pig (*Cavia porcellus*), rabbit (*Oryctolagus cuniculus*) and pika (*Ochotona princeps*). Sequences were aligned with Clustal Omega, conserved cCRE subregions were selected (yellow boxes) and putative transcription factor binding sites were identified using MEME (*71*). Sequence logos for motifs conserved across all species analyzed are shown (e.g. E2388481/enhD), along with those identified exclusively in gyrencephalic (e.g. E2388478/enhP) or lysencephalic species (e.g. E2388474/enhP). Top candidate transcription factors binding each motif, and their *p* value, are indicated. For each cCRE, the percent sequence identity histogram for gyrencephalic (red) and lysencephalic (green) species is plotted below the alignment overview.

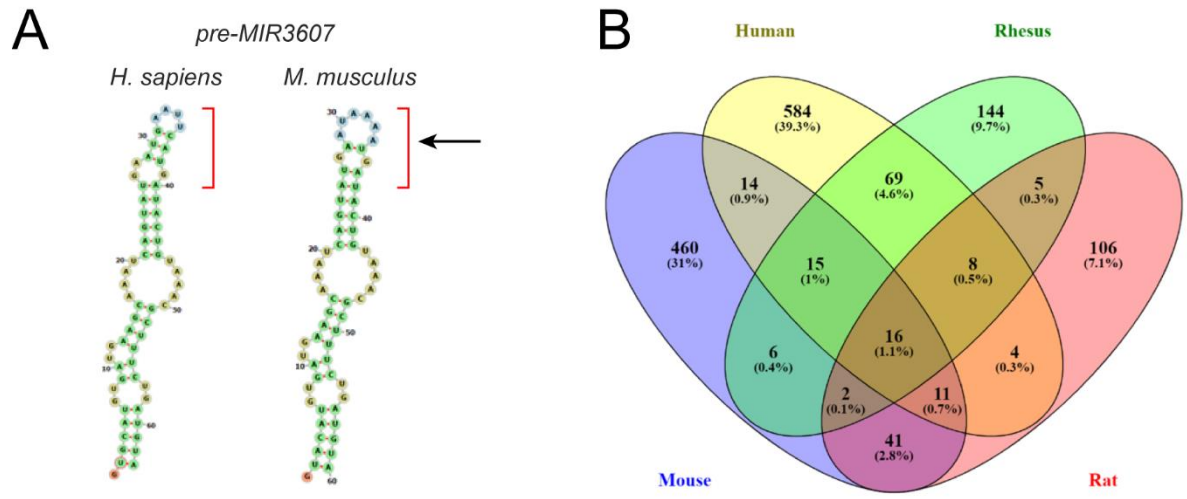

Fig. S8. Conservation and divergence of miRNAs targeting *APC*

(**A**) Schema of the predicted secondary structure of *pre-MIR3607* in human (*H. sapiens*) and mouse (*M. musculus*), according to (*61*). Sequence differences are predicted to affect the structure of the loop region (red brackets), shorter in mouse (arrow).

(**B**) Venn diagram of miRNAs computationally predicted to target *APC* in the indicated species. Intersections indicate the number and percentage of miRNAs common between the intersected species. Most targeting miRNAs are unique to each species, and the majority of common miRNAs are shared between primates (with a large and folded cortex), or between rodents (with a small and smooth cortex).

LEGENDS TO SUPPLEMENTARY TABLES

Supplementary Table S1. Sequence similarity of pre-*MIR3607* across mammals
Alignment of the sequence of pre-MIR3607 across mammalian species of main clades, spanning the 5p and 3p regions (green), and the loop region. Yellow shade indicates the seed sequence; purple shade indicates nucleotide mismatches compared to human (top); dashes indicate missing nucleotides.

Supplementary Table S2. Differential gene expression and functional enrichment analyses for RNAseq data between *MIR3607* and *Scrambled* conditions
Table parts contain: 1) Differential gene expression analysis (complete table without any filter: "FullTable"; table of significantly differentially expressed genes, padj. < 0.01, "FDR_0.01"). 2) Functional enrichment analysis with DAVID functional annotation clustering (DAVID defined default annotation categories for significant genes: "FDR_0.01_Full"; Gene Ontology for Biological Processes: "FDR_0.01_GOTERM_BP_ALL"; KEGG Pathway Ontology: "FDR_0.01_KEGG"; KEGG Pathway and Reactome Ontologies: "FDR_0.01_KEGG+Reactome"). 3) Cytoscape-ClueGo results for functionally grouped gene ontologies and pathway annotation networks ("ClueGO Results"). 4) MIR3607 human ortholog target genes ("HumanTargets"). 5) Differential gene expression results for predicted mouse *MIR3607* targets ("HumanOrthologTarget"). 6) GSEA enrichment analysis results (results for MSigDB Hallmark: "gsea_MSigDB_HALLMARK_H"; results for Gene Ontology, Biological Processes: "gsea_MsigDB_GO_BP_C5").

Supplementary Table S3. Target sites for *MIR3607* in the 3'UTR of *APC* across selected vertebrates
Identification and sequence of putative target sites for *MIR3607* in two locations of the *APC* mRNA 3'UTR. Green shade indicates identical sequence compared to human (top); dashes indicate missing nucleotides. Mouse and ferret are highlighted with red and yellow shades.

LEGENDS TO SUPPLEMENTARY MOVIES

Supplementary Movie S1. Radial migration of control mouse cortical neurons
Videomicrosopy of migrating cortical neurons in an organotypic slice culture from the cerebral cortex of an E17.5 mouse embryo electroporated *in utero* at E14.5 with DNA plasmids encoding for *Scrambled* miRNA, *mGFP-flox* and *Cre*. Ventricular surface is down, pial surface is up. The slice was prepared 20hr after *in utero* electroporation, and imaging started 4hrs after slice preparation. Time between frames is 30 min. Total imaging time is 24.5hrs. Red dots track three migrating neurons through the movie.

Supplementary Movie S2. Radial migration of *MIR3607*-overexpressing mouse cortical neurons
Videomicrosopy of migrating cortical neurons in an organotypic slice culture from the cerebral cortex of an E17.5 mouse embryo electroporated *in utero* at E14.5 with DNA plasmids encoding for *MIR3607*, *mGFP-flox* and *Cre*. Ventricular surface is down, pial surface is up. The slice was prepared 20hr after *in utero* electroporation, and imaging started 4hrs after slice preparation. Time between frames is 30 min. Total imaging time is 31.5hrs. Red dots track two migrating neurons through the movie.

REFERENCES AND NOTES

1. M. A. O'Leary, J. I. Bloch, J. J. Flynn, T. J. Gaudin, A. Giallombardo, N. P. Giannini, S. L. Goldberg, B. P. Kraatz, Z. X. Luo, J. Meng, X. Ni, M. J. Novacek, F. A. Perini, Z. S. Randall, G. W. Rougier, E. J. Sargis, M. T. Silcox, N. B. Simmons, M. Spaulding, P. M. Velazco, M. Weksler, J. R. Wible, A. L. Cirranello, The placental mammal ancestor and the post-K-Pg radiation of placentals. *Science* **339**, 662–667 (2013).

2. V. Borrell, I. Reillo, Emerging roles of neural stem cells in cerebral cortex development and evolution. *Dev. Neurobiol.* **72**, 955–971 (2012).

3. C. Dehay, H. Kennedy, Cell-cycle control and cortical development. *Nat. Rev. Neurosci.* **8**, 438–450 (2007).

4. V. Fernandez, C. Llinares-Benadero, V. Borrell, V. Fernández, C. Llinares-Benadero, V. Borrell, Cerebral cortex expansion and folding: What have we learned? *EMBO J.* **35**, 1021–1044 (2016).

5. I. T. Fiddes, G. A. Lodewijk, M. Mooring, C. M. Bosworth, A. D. Ewing, G. L. Mantalas, A. M. Novak, A. van den Bout, A. Bishara, J. L. Rosenkrantz, R. Lorig-Roach, A. R. Field, M. Haeussler, L. Russo, A. Bhaduri, T. J. Nowakowski, A. A. Pollen, M. L. Dougherty, X. Nuttle, M.-C. Addor, S. Zwolinski, S. Katzman, A. Kriegstein, E. E. Eichler, S. R. Salama, F. M. J. Jacobs, D. Haussler, Human-specific *NOTCH2NL* genes affect Notch signaling and cortical neurogenesis. *Cell* **173**, 1356–1369.e22 (2018).

6. M. Florio, V. Borrell, W. B. Huttner, Human-specific genomic signatures of neocortical expansion. *Curr. Opin. Neurobiol.* **42**, 33–44 (2017).

7. I. K. Suzuki, D. Gacquer, R. Van Heurck, D. Kumar, M. Wojno, A. Bilheu, A. Herpoel, N. Lambert, J. Cheron, F. Polleux, V. Detours, P. Vanderhaeghen, Human-specific NOTCH2NL genes expand cortical neurogenesis through Delta/Notch regulation. *Cell* **173**, 1370–1384.e16 (2018).

8. A. Cárdenas, A. Villalba, C. de Juan Romero, E. Picó, C. Kyrousi, A. C. Tzika, M. Tessier-Lavigne, L. Ma, M. Drukker, S. Cappello, V. Borrell, Evolution of cortical neurogenesis in amniotes controlled by Robo signaling levels. *Cell* **174**, 590–606.e21 (2018).

9. I. Kelava, E. Lewitus, W. B. Huttner, The secondary loss of gyrencephaly as an example of evolutionary phenotypical reversal. *Front. Neuroanat.* **7**, 16 (2013).

10. A. Villalba, M. Götz, V. Borrell, in *Current Topics in Developmental Biology* (Academic Press Inc., 2021), vol. 142, pp. 1–66.

11. E. Taverna, M. Götz, W. B. Huttner, The cell biology of neurogenesis: Toward an understanding of the development and evolution of the neocortex. *Annu. Rev. Cell Dev. Biol.* **30**, 465–502 (2014).

12. I. Reillo, V. V. Borrell, Germinal zones in the developing cerebral cortex of ferret: Ontogeny, cell cycle kinetics, and diversity of progenitors. *Cereb. Cortex* **22**, 2039–2054 (2012).

13. I. Reillo, C. De Juan Romero, M. Á. García-Cabezas, V. Borrell, A role for intermediate radial glia in the tangential expansion of the mammalian cerebral cortex. *Cereb. Cortex* **21**, 1674–1694 (2011).

14. D. V. Hansen, J. H. Lui, P. R. L. L. Parker, A. R. Kriegstein, Neurogenic radial glia in the outer subventricular zone of human neocortex. *Nature* **464**, 554–561 (2010).

15. S. A. Fietz, I. Kelava, J. Vogt, M. Wilsch-Brauninger, D. Stenzel, J. L. Fish, D. Corbeil, A. Riehn, W. Distler, R. Nitsch, W. B. Huttner, M. Wilsch-Bräuninger, D. Stenzel, J. L. Fish, D. Corbeil, A. Riehn, W. Distler, R. Nitsch, W. B. Huttner, OSVZ progenitors of human and ferret neocortex are epithelial-like and expand by integrin signaling. *Nat. Neurosci.* **13**, 690–699 (2010).

16. I. H. M. Smart, C. Dehay, P. Giroud, M. Berland, H. Kennedy, Unique morphological features of the proliferative zones and postmitotic compartments of the neural epithelium giving rise to striate and extrastriate cortex in the monkey. *Cereb. Cortex* **12**, 37–53 (2002).

17. V. Borrell, M. Götz, Role of radial glial cells in cerebral cortex folding. *Curr. Opin. Neurobiol.* **27**, 39–46 (2014).

18. P. Rakic, A small step for the cell, a giant leap for mankind: A hypothesis of neocortical expansion during evolution. *Trends Neurosci.* **18**, 383–388 (1995).

19. M. Florio, M. Heide, A. Pinson, H. Brandl, M. Albert, S. Winkler, P. Wimberger, W. B. Huttner, M. Hiller, Evolution and cell-type specificity of human-specific genes preferentially expressed in progenitors of fetal neocortex. *eLife* **7**, e32332 (2018).

20. M. L. Arcila, M. Betizeau, X. A. Cambronne, E. Guzman, N. Doerflinger, F. Bouhallier, H. Zhou, B. Wu, N. Rani, D. S. Bassett, U. Borello, C. Huissoud, R. H. Goodman, C. Dehay, K. S. Kosik, Novel primate miRNAs coevolved with ancient target genes in germinal zone-specific expression patterns. *Neuron* **81**, 1255–1262 (2014).

21. T. J. Nowakowski, N. Rani, M. Golkaram, H. R. Zhou, B. Alvarado, K. Huch, J. A. West, A. Leyrat, A. A. Pollen, A. R. Kriegstein, L. R. Petzold, K. S. Kosik, Regulation of cell-type-specific transcriptomes by microRNA networks during human brain development. *Nat. Neurosci.* **21**, 1784–1792 (2018).

22. S. A. Fietz, R. Lachmann, H. Brandl, M. Kircher, N. Samusik, R. Schröder, N. Lakshmanaperumal, I. Henry, J. Vogt, A. Riehn, W. Distler, R. Nitsch, W. Enard, S. Pääbo, W. B. Huttner, R. Schroder, N. Lakshmanaperumal, I. Henry, J. Vogt, A. Riehn, W. Distler, R. Nitsch, W. Enard, S. Paabo, W. B. Huttner, Transcriptomes of germinal zones of human and mouse fetal neocortex suggest a role of extracellular matrix in progenitor self-renewal. *Proc. Natl. Acad. Sci. U.S.A.* **109**, 11836–11841 (2012).

23. M. Á. Martínez-Martínez, C. De Juan Romero, V. Fernández, A. Cárdenas, M. Götz, V. Borrell, A restricted period for formation of outer subventricular zone defined by Cdh1 and Trnp1 levels. *Nat. Commun.* **7**, 11812 (2016).

24. C. de Juan Romero, V. Borrell, Genetic maps and patterns of cerebral cortex folding. *Curr. Opin. Cell Biol.* **49**, 31–37 (2017).

25. C. Llinares-Benadero, V. Borrell, Deconstructing cortical folding: Genetic, cellular and mechanical determinants. *Nat. Rev. Neurosci.* **20**, 161–176 (2019).

26. C. De Juan Romero, C. Bruder, U. Tomasello, J. M. Sanz-Anquela, V. V. Borrell, J. M. Sanz-Anquela, V. V. Borrell, Discrete domains of gene expression in germinal layers distinguish the development of gyrencephaly. *EMBO J.* **34**, 1859–1874 (2015).

27. S. Pati, N. E. Supeno, S. Muthuraju, R. Abdul Hadi, A. R. I. Ghani, F. M. Idris, M. Maletic-Savatic, J. M. Abdullah, H. Jaafar, MicroRNA profiling reveals unique miRNA signatures in IGF-1 treated embryonic striatal stem cell fate decisions in striatal neurogenesis in vitro. *Biomed. Res. Int.* **2014**, 1–14 (2014).

28. L. F. R. Gebert, I. J. MacRae, Regulation of microRNA function in animals. *Nat. Rev. Mol. Cell Biol.* **20**, 21–37 (2019).

29. C. Englund, A. Fink, C. Lau, D. Pham, R. A. M. Daza, A. Bulfone, T. Kowalczyk, R. F. Hevner, Pax6, Tbr2, and Tbr1 are expressed sequentially by radial glia, intermediate progenitor cells, and postmitotic neurons in developing neocortex. *J. Neurosci.* **25**, 247–251 (2005).

30. M. Betizeau, V. Cortay, D. Patti, S. Pfister, E. Gautier, A. Bellemin-Ménard, M. Afanassieff, C. Huissoud, R. J. Douglas, H. Kennedy, C. Dehay, Precursor diversity and complexity of lineage relationships in the outer subventricular zone of the primate. *Neuron* **80**, 442–457 (2013).

31. M. Á. Martínez-Martínez, G. Ciceri, A. Espinós, V. Fernández, O. Marín, V. Borrell, Extensive branching of radially-migrating neurons in the mammalian cerebral cortex. *J. Comp. Neurol.* **527**, 1558–1576 (2019).

32. H. Tabata, K. Nakajima, Multipolar migration: The third mode of radial neuronal migration in the developing cerebral cortex. *J. Neurosci.* **23**, 9996–10001 (2003).

33. A. Chenn, C. A. Walsh, Regulation of cerebral cortical size by control of cell cycle exit in neural precursors. *Science* **297**, 365–369 (2002).

34. A. Herrera, M. Saade, A. Menendez, E. Marti, S. Pons, Sustained Wnt/β-catenin signalling causes neuroepithelial aberrations through the accumulation of aPKC at the apical pole. *Nat. Commun.* **5**, 4168 (2014).

35. G. J. Woodhead, C. A. Mutch, E. C. Olson, A. Chenn, Cell-autonomous beta-catenin signaling regulates cortical precursor proliferation. *J. Neurosci.* **26**, 12620–12630 (2006).

36. Y. Lin, Q. Gu, Z. Sun, B. Sheng, C. Qi, B. Liu, T. Fu, C. Liu, Y. Zhang, Upregulation of miR-3607 promotes lung adenocarcinoma proliferation by suppressing APC expression. *Biomed. Pharmacother.* **95**, 497–503 (2017).

37. J. Yoo, R. J. Hajjar, D. Jeong, Generation of efficient miRNA inhibitors using tough decoy constructs. *Methods Mol. Biol.* **1521**, 41–53(2017).

38. O. Machon, C. J. van den Bout, M. Backman, R. Kemler, S. Krauss, Role of beta-catenin in the developing cortical and hippocampal neuroepithelium. *Neuroscience* **122**, 129–143 (2003).

39. X. Wang, J.-W. W. Tsai, B. LaMonica, A. R. Kriegstein, A new subtype of progenitor cell in the mouse embryonic neocortex. *Nat. Neurosci.* **14**, 555–561 (2011).

40. M. Florio, M. Albert, E. Taverna, T. Namba, H. Brandl, E. Lewitus, C. Haffner, A. Sykes, F. K. Wong, J. Peters, E. Guhr, S. Klemroth, K. Prufer, J. Kelso, R. Naumann, I. Nusslein, A. Dahl, R. Lachmann, S. Paabo, W. B. Huttner, Human-specific gene *ARHGAP11B* promotes basal progenitor amplification and neocortex expansion. *Science* **347**, 1465–1470 (2015).

41. J. L. Boyd, S. L. Skove, J. P. Rouanet, L. J. Pilaz, T. Bepler, R. Gordân, G. A. Wray, D. L. Silver, Human-chimpanzee differences in a FZD8 enhancer alter cell-cycle dynamics in the developing neocortex. *Curr. Biol.* **25**, 772–779 (2015).

42. L. M. Farkas, C. Haffner, T. Giger, P. Khaitovich, K. Nowick, C. Birchmeier, S. Pääbo, W. B. Huttner, Insulinoma-associated 1 has a panneurogenic role and promotes the generation and expansion of basal progenitors in the developing mouse neocortex. *Neuron* **60**, 40–55 (2008).

43. T. Mukhtar, J. Breda, A. Grison, Z. Karimaddini, P. Grobecker, D. Iber, C. Beisel, E. van Nimwegen, V. Taylor, Tead transcription factors differentially regulate cortical development. *Sci. Rep.* **10**, 4625 (2020).

44. U. Borello, B. Berarducci, E. Delahaye, D. J. Price, C. Dehay, SP8 transcriptional regulation of *Cyclin D1* during mouse early corticogenesis. *Front. Neurosci.* **12**, 119 (2018).

45. C. N. Wrobel, C. A. Mutch, S. Swaminathan, M. M. Taketo, A. Chenn, Persistent expression of stabilized β-catenin delays maturation of radial glial cells into intermediate progenitors. *Dev. Biol.* **309**, 285–297 (2007).

46. R. S. Schmid, P. F. Maness, L1 and NCAM adhesion molecules as signaling coreceptors in neuronal migration and process outgrowth. *Curr. Opin. Neurobiol.* **18**, 245–250 (2008).

47. C. A. Mutch, N. Funatsu, E. S. Monuki, A. Chenn, β-Catenin signaling levels in progenitors influence the laminar cell fates of projection neurons. *J. Neurosci.* **29**, 13710–13719 (2009).

48. Y. Yokota, W. Y. Kim, Y. Chen, X. Wang, A. Stanco, Y. Komuro, W. Snider, E. S. Anton, The adenomatous polyposis coli protein is an essential regulator of radial glial polarity and construction of the cerebral cortex. *Neuron* **61**, 42–56 (2009).

49. N. Nakagawa, J. Li, K. Yabuno-Nakagawa, T. Y. Eom, M. Cowles, T. Mapp, R. Taylor, E. S. Anton, APC sets the Wnt tone necessary for cerebral cortical progenitor development. *Genes Dev.* **31**, 1679–1692 (2017).

50. A. Prieto-Colomina, V. Fernández, K. Chinnappa, V. Borrell, MiRNAs in early brain development and pediatric cancer. *Bioessays* **43**, e2100073 (2021).

51. V. Fernández, M. Á. Martínez-Martínez, A. Prieto-Colomina, A. Cárdenas, R. Soler, M. Dori, U. Tomasello, Y. Nomura, J. P. López-Atalaya, F. Calegari, V. Borrell, Repression of Irs2 by let-7 miRNAs is essential for homeostasis of the telencephalic neuroepithelium. *EMBO J.* **39**, e105479 (2020).

52. T. Haraguchi, Y. Ozaki, H. Iba, Vectors expressing efficient RNA decoys achieve the long-term suppression of specific microRNA activity in mammalian cells. *Nucleic Acids Res.* **37**, e43 (2009).

53. V. Borrell, A. Cárdenas, G. Ciceri, J. Galcerán, N. Flames, R. Pla, S. Nóbrega-Pereira, C. García-Frigola, S. Peregrín, Z. Zhao, L. Ma, M. Tessier-Lavigne, O. Marín, Slit/Robo signaling modulates the proliferation of central nervous system progenitors. *Neuron* **76**, 338–352 (2012).

54. M. A. Lancaster, J. A. Knoblich, Generation of cerebral organoids from human pluripotent stem cells. *Nat. Protoc.* **9**, 2329–2340 (2014).

55. D. De Pietri Tonelli, J. N. Pulvers, C. Haffner, E. P. Murchison, G. J. Hannon, W. B. Huttner, miRNAs are essential for survival and differentiation of newborn neurons but not for expansion of neural progenitors during early neurogenesis in the mouse embryonic neocortex. *Development* **135**, 3911–3921 (2008).

56. S. T. Sherry, M. Ward, K. Sirotkin, dbSNP—Database for single nucleotide polymorphisms and other classes of minor genetic variation. *Genome Res.* **9**, 677–679 (1999).

57. J. T. Robinson, H. Thorvaldsdottir, W. Winckler, M. Guttman, E. S. Lander, G. Getz, J. P. Mesirov, Integrative genomics viewer. *Nat. Biotechnol.* **29**, 24–26 (2011).

58. G. Yu, L.-G. Wang, Y. Han, Q.-Y. He, clusterProfiler: An R package for comparing biological themes among gene clusters. *OMICS* **16**, 284–287 (2012).

59. E. I. Boyle, S. Weng, J. Gollub, H. Jin, D. Botstein, J. M. Cherry, G. Sherlock, GO::TermFinder—Open source software for accessing Gene Ontology information and finding significantly enriched Gene Ontology terms associated with a list of genes. *Bioinformatics* **20**, 3710–3715 (2004).

60. A. Subramanian, P. Tamayo, V. K. Mootha, S. Mukherjee, B. L. Ebert, M. A. Gillette, A. Paulovich, S. L. Pomeroy, T. R. Golub, E. S. Lander, J. P. Mesirov, Gene set enrichment

analysis: A knowledge-based approach for interpreting genome-wide expression profiles. *Proc. Natl. Acad. Sci. U.S.A.* **102**, 15545–15550 (2005).

61. K. Sato, M. Akiyama, Y. Sakakibara, RNA secondary structure prediction using deep learning with thermodynamic integration. *Nat. Commun.* **12**, 941 (2021).

62. D. Karolchik, A. S. Hinrichs, T. S. Furey, K. M. Roskin, C. W. Sugnet, D. Haussler, W. J. Kent, The UCSC Table Browser data retrieval tool. *Nucleic Acids Res.* **32**, D493–D496 (2004).

63. F. Madeira, Y. Park, J. Lee, N. Buso, T. Gur, N. Madhusoodanan, P. Basutkar, A. Tivey, S. Potter, R. Finn, R. Lopez, The EMBL-EBI search and sequence analysis tools APIs in 2019. *Nucleic Acids Res.* **47**, W636–W641 (2019).

64. A. M. Waterhouse, J. B. Procter, D. M. A. Martin, M. Clamp, G. J. Barton, Jalview Version 2—A multiple sequence alignment editor and analysis workbench. *Bioinformatics* **25**, 1189–1191 (2009).

65. N. A. O'Leary, M. W. Wright, J. R. Brister, S. Ciufo, D. Haddad, R. McVeigh, B. Rajput, B. Robbertse, B. Smith-White, D. Ako-Adjei, A. Astashyn, A. Badretdin, Y. Bao, O. Blinkova, V. Brover, V. Chetvernin, J. Choi, E. Cox, O. Ermolaeva, C. M. Farrell, T. Goldfarb, T. Gupta, D. Haft, E. Hatcher, W. Hlavina, V. S. Joardar, V. K. Kodali, W. Li, D. Maglott, P. Masterson, K. M. McGarvey, M. R. Murphy, K. O'Neill, S. Pujar, S. H. Rangwala, D. Rausch, L. D. Riddick, C. Schoch, A. Shkeda, S. S. Storz, H. Sun, F. Thibaud-Nissen, I. Tolstoy, R. E. Tully, A. R. Vatsan, C. Wallin, D. Webb, W. Wu, M. J. Landrum, A. Kimchi, T. Tatusova, M. DiCuccio, P. Kitts, T. D. Murphy, K. D. Pruitt, Reference sequence (RefSeq) database at NCBI: Current status, taxonomic expansion, and functional annotation. *Nucleic Acids Res.* **44**, D733–D745 (2016).

66. J. Navarro Gonzalez, A. S. Zweig, M. L. Speir, D. Schmelter, K. R. Rosenbloom, B. J. Raney, C. C. Powell, L. R. Nassar, N. D. Maulding, C. M. Lee, B. T. Lee, A. S. Hinrichs, A. C. Fyfe, J. D. Fernandes, M. Diekhans, H. Clawson, J. Casper, A. Benet-Pagès, G. P. Barber,

D. Haussler, R. M. Kuhn, M. Haeussler, W. J. Kent, The UCSC Genome Browser database: 2021 update. *Nucleic Acids Res.* **49**, D1046–D1057 (2021).

67. F. Abascal, R. Acosta, N. J. Addleman, J. Adrian, V. Afzal, B. Aken, J. A. Akiyama, O. Al Jammal, H. Amrhein, S. M. Anderson, G. R. Andrews, I. Antoshechkin, K. G. Ardlie, J. Armstrong, M. Astley, B. Banerjee, A. A. Barkal, I. H. A. Barnes, I. Barozzi, D. Barrell, G. Barson, D. Bates, U. K. Baymuradov, C. Bazile, M. A. Beer, S. Beik, M. A. Bender, R. Bennett, L. P. B. Bouvrette, B. E. Bernstein, A. Berry, A. Bhaskar, A. Bignell, S. M. Blue, D. M. Bodine, C. Boix, N. Boley, T. Borrman, B. Borsari, A. P. Boyle, L. A. Brandsmeier, A. Breschi, E. H. Bresnick, J. A. Brooks, M. Buckley, C. B. Burge, R. Byron, E. Cahill, L. Cai, L. Cao, M. Carty, R. G. Castanon, A. Castillo, H. Chaib, E. T. Chan, D. R. Chee, S. Chee, H. Chen, H. Chen, J. Y. Chen, S. Chen, J. M. Cherry, S. B. Chhetri, J. S. Choudhary, J. Chrast, D. Chung, D. Clarke, N. A. L. Cody, C. J. Coppola, J. Coursen, A. M. D'Ippolito, S. Dalton, C. Danyko, C. Davidson, J. Davila-Velderrain, C. A. Davis, J. Dekker, A. Deran, G. DeSalvo, G. Despacio-Reyes, C. N. Dewey, D. E. Dickel, M. Diegel, M. Diekhans, V. Dileep, B. Ding, S. Djebali, A. Dobin, D. Dominguez, S. Donaldson, J. Drenkow, T. R. Dreszer, Y. Drier, M. O. Duff, D. Dunn, C. Eastman, J. R. Ecker, M. D. Edwards, N. El-Ali, S. I. Elhajjajy, K. Elkins, A. Emili, C. B. Epstein, R. C. Evans, I. Ezkurdia, K. Fan, P. J. Farnham, N. P. Farrell, E. A. Feingold, A. M. Ferreira, K. Fisher-Aylor, S. Fitzgerald, P. Flicek, C. S. Foo, K. Fortier, A. Frankish, P. Freese, S. Fu, X. D. Fu, Y. Fu, Y. Fukuda-Yuzawa, M. Fulciniti, A. P. W. Funnell, I. Gabdank, T. Galeev, M. Gao, C. G. Giron, T. H. Garvin, C. A. Gelboin-Burkhart, G. Georgolopoulos, M. B. Gerstein, B. M. Giardine, D. K. Gifford, D. M. Gilbert, D. A. Gilchrist, S. Gillespie, T. R. Gingeras, P. Gong, A. Gonzalez, J. M. Gonzalez, P. Good, A. Goren, D. U. Gorkin, B. R. Graveley, M. Gray, J. F. Greenblatt, E. Griffiths, M. T. Groudine, F. Grubert, M. Gu, R. Guigó, H. Guo, Y. Guo, Y. Guo, G. Gursoy, M. Gutierrez-Arcelus, J. Halow, R. C. Hardison, M. Hardy, M. Hariharan, A. Harmanci, A. Harrington, J. L. Harrow, T. B. Hashimoto, R. D. Hasz, M. Hatan, E. Haugen, J. E. Hayes, P. He, Y. He, N. Heidari, D. Hendrickson, E. F. Heuston, J. A. Hilton, B. C. Hitz, A. Hochman, C. Holgren, L. Hou, S. Hou, Y. H. E. Hsiao, S. Hsu, H. Huang, T. J. Hubbard, J. Huey, T. R. Hughes, T. Hunt, S. Ibarrientos, R. Issner, M. Iwata, O. Izuogu, T. Jaakkola, N. Jameel, C. Jansen, L. Jiang, P. Jiang, A. Johnson, R. Johnson, I. Jungreis, M. Kadaba, M. Kasowski, M.

Kasparian, M. Kato, R. Kaul, T. Kawli, M. Kay, J. C. Keen, S. Keles, C. A. Keller, D. Kelley, M. Kellis, P. Kheradpour, D. S. Kim, A. Kirilusha, R. J. Klein, B. Knoechel, S. Kuan, M. J. Kulik, S. Kumar, A. Kundaje, T. Kutyavin, J. Lagarde, B. R. Lajoie, N. J. Lambert, J. Lazar, A. Y. Lee, D. Lee, E. Lee, J. W. Lee, K. Lee, C. S. Leslie, S. Levy, B. Li, H. Li, N. Li, X. Li, Y. I. Li, Y. Li, Y. Li, Y. Li, J. Lian, M. W. Libbrecht, S. Lin, Y. Lin, D. Liu, J. Liu, P. Liu, T. Liu, X. S. Liu, Y. Liu, Y. Liu, M. Long, S. Lou, J. Loveland, A. Lu, Y. Lu, E. Lécuyer, L. Ma, M. Mackiewicz, B. J. Mannion, M. Mannstadt, D. Manthravadi, G. K. Marinov, F. J. Martin, E. Mattei, K. McCue, M. McEown, G. McVicker, S. K. Meadows, A. Meissner, E. M. Mendenhall, C. L. Messer, W. Meuleman, C. Meyer, S. Miller, M. G. Milton, T. Mishra, D. E. Moore, H. M. Moore, J. E. Moore, S. H. Moore, J. Moran, A. Mortazavi, J. M. Mudge, N. Munshi, R. Murad, R. M. Myers, V. Nandakumar, P. Nandi, A. M. Narasimha, A. K. Narayanan, H. Naughton, F. C. P. Navarro, P. Navas, J. Nazarovs, J. Nelson, S. Neph, F. J. Neri, J. R. Nery, A. R. Nesmith, J. S. Newberry, K. M. Newberry, V. Ngo, R. Nguyen, T. B. Nguyen, T. Nguyen, A. Nishida, W. S. Noble, C. S. Novak, E. M. Novoa, B. Nuñez, C. W. O'Donnell, S. Olson, K. C. Onate, E. Otterman, H. Ozadam, M. Pagan, T. Palden, X. Pan, Y. Park, E. C. Partridge, B. Paten, F. Pauli-Behn, M. J. Pazin, B. Pei, L. A. Pennacchio, A. R. Perez, E. H. Perry, D. D. Pervouchine, N. N. Phalke, Q. Pham, D. H. Phanstiel, I. Plajzer-Frick, G. A. Pratt, H. E. Pratt, S. Preissl, J. K. Pritchard, Y. Pritykin, M. J. Purcaro, Q. Qin, G. Quinones-Valdez, I. Rabano, E. Radovani, A. Raj, N. Rajagopal, O. Ram, L. Ramirez, R. N. Ramirez, D. Rausch, S. Raychaudhuri, J. Raymond, R. Razavi, T. E. Reddy, T. M. Reimonn, B. Ren, A. Reymond, A. Reynolds, S. K. Rhie, J. Rinn, M. Rivera, J. C. Rivera-Mulia, B. S. Roberts, J. M. Rodriguez, J. Rozowsky, R. Ryan, E. Rynes, D. N. Salins, R. Sandstrom, T. Sasaki, S. Sathe, D. Savic, A. Scavelli, J. Scheiman, C. Schlaffner, J. A. Schloss, F. W. Schmitges, L. H. See, A. Sethi, M. Setty, A. Shafer, S. Shan, E. Sharon, Q. Shen, Y. Shen, R. I. Sherwood, M. Shi, S. Shin, N. Shoresh, K. Siebenthall, C. Sisu, T. Slifer, C. A. Sloan, A. Smith, V. Snetkova, M. P. Snyder, D. V. Spacek, S. Srinivasan, R. Srivas, G. Stamatoyannopoulos, J. A. Stamatoyannopoulos, R. Stanton, D. Steffan, S. Stehling-Sun, J. S. Strattan, A. Su, B. Sundararaman, M. M. Suner, T. Syed, M. Szynkarek, F. Y. Tanaka, D. Tenen, M. Teng, J. A. Thomas, D. Toffey, M. L. Tress, D. E. Trout, G. Trynka, J. Tsuji, S. A. Upchurch, O. Ursu, B. Uszczynska-Ratajczak, M. C. Uziel, A. Valencia, B. Van Biber, A. G. van der Velde, E. L. Van Nostrand, Y. Vaydylevich, J.

Vazquez, A. Victorsen, J. Vielmetter, J. Vierstra, A. Visel, A. Vlasova, C. M. Vockley, S. Volpi, S. Vong, H. Wang, M. Wang, Q. Wang, R. Wang, T. Wang, W. Wang, X. Wang, Y. Wang, N. K. Watson, X. Wei, Z. Wei, H. Weisser, S. M. Weissman, R. Welch, R. E. Welikson, Z. Weng, H. J. Westra, J. W. Whitaker, C. White, K. P. White, A. Wildberg, B. A. Williams, D. Wine, H. N. Witt, B. Wold, M. Wolf, J. Wright, R. Xiao, X. Xiao, J. Xu, K. K. Yan, Y. Yan, H. Yang, X. Yang, Y. W. Yang, G. G. Yardimci, B. A. Yee, G. W. Yeo, T. Young, T. Yu, F. Yue, C. Zaleski, C. Zang, H. Zeng, W. Zeng, D. R. Zerbino, J. Zhai, L. Zhan, Y. Zhan, B. Zhang, J. Zhang, J. Zhang, K. Zhang, L. Zhang, P. Zhang, Q. Zhang, X. O. Zhang, Y. Zhang, Z. Zhang, Y. Zhao, Y. Zheng, G. Zhong, X. Q. Zhou, Y. Zhu, J. Zimmerman, Expanded encyclopaedias of DNA elements in the human and mouse genomes. *Nature* **583**, 699–710 (2020).

68. T. L. Bailey, J. Johnson, C. E. Grant, W. S. Noble, The MEME Suite. *Nucleic Acids Res.* **43**, W39–W49 (2015).

69. L. Shi, X. Luo, J. Jiang, Y. Chen, C. Liu, T. Hu, M. Li, Q. Lin, Y. Li, J. Huang, H. Wang, Y. Niu, Y. Shi, M. Styner, J. Wang, Y. Lu, X. Sun, H. Yu, W. Ji, B. Su, Transgenic rhesus monkeys carrying the human MCPH1 gene copies show human-like neoteny of brain development. *Natl. Sci. Rev.* **6**, 480–493 (2019).

70. M. B. Johnson, X. Sun, A. Kodani, R. Borges-Monroy, K. M. Girskis, S. C. Ryu, P. P. Wang, K. Patel, D. M. Gonzalez, Y. M. Woo, Z. Yan, B. Liang, R. S. Smith, M. Chatterjee, D. Coman, X. Papademetris, L. H. Staib, F. Hyder, J. B. Mandeville, P. E. Grant, K. Im, H. Kwak, J. F. Engelhardt, C. A. Walsh, B. I. Bae, Aspm knockoutferret reveals an evolutionary mechanism governing cerebral cortical size. *Nature* **556**, 370–375 (2018).

71. T. Bailey, C. Elkan, Fitting a mixture model by expectation maximization to discover motifs in biopolymers. *Proc. Int. Conf. Intell. Syst. Mol. Biol.* **2**, 28–36 (1994).